GeoScienceWorld
Lithosphere
Volume 2021, Article ID 5992165, 15 pages
https://doi.org/10.2113/2021/5992165

Lithosphere

Research Article

Quantitative Interpretation of Water Sensitivity Based on Well Log Data: A Case of a Conglomerate Reservoir in the Karamay Oil Field

Lingxuan Jin,[1,2] **Yuming Liu**,[1,2] **Jian Gao**,[3] **and Ziqiang Hao**[1,2]

[1]*State Key Laboratory of Petroleum Resources and Prospecting, China University of Petroleum, Beijing 102249, China*
[2]*College of Geosciences, China University of Petroleum, Beijing 102249, China*
[3]*Enhanced Oil Recovery Research Center, PetroChina Research Institute of Petroleum Exploration and Development, Beijing 100083, China*

Correspondence should be addressed to Yuming Liu; liuym@cup.edu.cn

Received 10 May 2021; Accepted 24 September 2021; Published 23 October 2021

Academic Editor: Shiyuan Zhan

In the process of oil reservoir development, clay minerals in the pores of a reservoir swell because of water absorption, blocking the pore channels, and decreasing the reservoir permeability. This phenomenon is referred to as reservoir water sensitivity. To develop and protect oil and gas fields more scientifically and effectively and save development cost, we examine the water sensitivity of the low-permeability conglomerate reservoir of the Lower Karamay Formation in the 530-well area of District 8 of the Karamay oil field. Based on multiple linear regression and neural network methods, the quantitative calculation of different types of clay minerals was performed by comprehensively using natural gamma ray, neutron, density, sonic transit time, and X-ray diffraction (XRD) analysis data. The water sensitivity experiment was performed in the study area, and the logging interpretation method of reservoir water sensitivity was established by considering the clay mineral content as the medium; moreover, the reservoir water sensitivity degree was quantitatively explained.

1. Introduction

Water sensitivity is a phenomenon as per which the permeability of an aqueous medium-containing clay minerals decreases when extraneous solutions with different mineral concentrations displace each other from the formation fluid [1–3]. For developing oil fields, reservoir water sensitivity can damage reservoirs [4]. This can lead to difficulties in forming energy supplements, such as water injection and gas injection, and can reduce reservoir productivity, thus indicating it may have strong negative effects on development. Therefore, it is necessary to investigate water sensitivity.

In the oil and gas industry, reservoir water sensitivity damage is an important problem often encountered [5, 6]. In 1950s, researchers used core flow experiments to examine formation damage because of clay expansion. In the 1970s, the influence of oil layer protection expanded; since 1974, the USA has held a conference on preventing formation damage to discuss important technical issues such as reservoir protection [7]. Valdya [8] examined changes in fluid acidity and basicity, in addition to the effect of ion exchange on particle migration and the resultant strong formation damage. Based on results regarding the types and causes of reservoir damage, Bishop [9] proposed the formation damage index (FDI), which can reflect the degree of formation sensitivity damage. After 1990s, when multiple technologies for oil layer protection were developed, a number of researchers used core analyses such as X-ray diffraction (XRD) experiments to intuitively obtain clay data [10, 11]. However, in oil field production areas, core data are extremely limited, and there is a greater amount of log data. Thus, some scholars have attempted to use log data to examine the presence of clay minerals and examine the reservoir water sensitivity [12].

Previously, experts used the traditional Schlumberger clay mineral interpretation map, which identifies clay minerals based on differences in the levels of U, Th, and K reported in different types of clay [13]. However, for many areas, no natural gamma ray spectral data are available. For cases in which only conventional log curves can be obtained, researchers previously established a theoretical model of typical sand and mudstone using a neutron-density cross plot that can be used to determine both the content of clay minerals and their distribution [14]. As per the abovementioned methods, natural gamma ray spectral data and neutron density log data are related to the content and type of clay minerals, indicating that a clay mineral log interpretation model can be established using multiple linear regression [15–17]. If the linear relation is unideal, a nonlinear NN method can be used to establish an interpretation model [18–20].

Well log data are the average value of certain physical quantities in the rock medium detected by the logging instrument, e.g., the volume density of the rock can be considered as the average density of the rock medium (rock solid skeleton and fluid) in the detection range of the density logging tool. Sonic transit time can be considered as the average value of the sonic transit time of multiple rock components (rock solid skeleton and fluid) on the sound wave propagation path. Other log data, such as hydrogen index, rock natural radioactivity intensity, thermal neutron macroscopic capture cross section, and photoelectric absorption cross section, can be similarly approximated. In this study, we use these log data to establish an approximate mathematical model on the relation between log measurement results (physical) and rock geological parameters (relative volume) to clearly reflect the physical characteristics of reservoirs. Moreover, this model can be referred to as a logging response volume model [21].

When only conventional log data are available, the determination of log values on the tri-porosity (sonic, neutron, and density) of dry clay as per the sonic, neutron, and density log response equations is important for forming a rock volume physical model with other known parameters. For example, lower dry clay density, higher sonic transit time, and higher neutron value led to a lower total porosity in the formation [22]. Water sensitivity refers to the phenomenon as per which the content of each clay mineral in the reservoir affects changes in the physical properties of the reservoir. Therefore, we can use tri-porosity log data to interpret clay minerals to clearly reflect the physical characteristics of water-sensitive reservoirs.

Because clay types vary with depth, the log values of continuous depth reflect the comprehensive responses of dry clay, skeleton minerals (such as quartz), and pore fluids. Therefore, compared with actual values, the final sonic, neutron, and density values of dry clay may have a large error, which will considerably affect the evaluation accuracy of porosity and oil and gas saturation, in addition to regional geological understanding and technical decision-making of explorers. Therefore, the logging parameters of dry clay tri-porosity should be obtained by calculation to continue research and reduce the error of total porosity calculations.

In this study, we applied tri-porosity log interpretation data to examine clay minerals in the low-permeability conglomerate reservoir of the Lower Karamay Formation in the 530-well area of District 8 of the Karamay oil field for research verification. We reported that this data have a significant level of applicability and provide a method for improving the log evaluation of clay minerals in reservoirs.

2. Overview of the Study Area

The Lower Karamay Formation in the 530-well area of District 8 of the Karamay oil field is located in the northwestern margin of Junggar Basin at the footwall of the South Baijiantan Fault and the Ke-Wu fault (Figure 1; [23]). The top surface structure of the reservoir is a northwest–southeast monocline. Under the traction of thrust fault, the dip angle of strata close to the northwest fault reaches 45°; furthermore, the dip angle of strata in the southeast slope area is between 3° and 5° (Figure 2).

The area we select to examine is located in the southeast extended area. Gradually, the plane thickens from northwest to southeast and can be longitudinally divided into 5 sand layers and 14 single-sand layers. The lithology of the area is primarily glutenite and conglomerate with an average porosity of 10.6% and an average permeability of 6.1 mD [23], thus making it a low-porosity and low-permeability reservoir. The considerable difference between the coefficient of variation and the coefficient of burst indicates that the reservoir is considerably heterogeneous. In this area, the Lower Karamay Formation is a fan delta facies deposit. The sedimentary thickness is between 150 and 190 m, the average thickness is 175 m [24], the containing area is 2.6 km^2, and the geological reserves are 192.7×10^4 t.

Previously, researchers established a complete set of stratigraphic sequences in the northwest, south, and east of the Qigar Basin via detailed research on the geological conditions of the basin. The reservoir sedimentary thickness of the Lower Karamay Formation in District 8 of this oil field is between 46 and 221 m with an average thickness of 165 m. Gradually, the plane thickens from northwest to southeast, and the reservoir has two sets of sand groups, S_7 and S_6, on the bottom and top, respectively. The primary sand layer is S_7, whereas the sand groups studied are S_7^3, S_7^4, and S_7^5. Each layer can be subdivided into four to five smaller layers, and Well K484 is shown as an example (Figure 3).

Currently, the reservoir has entered the high water-cut period development stage. Based on the rerecognition of its geology, the block is suffering from various problems, including serious underinjection of water wells, poor efficiency of oil wells, rapid rise in water cut, and significant decline in production. Because of the water sensitivity of the reservoir, there is a large gap between the daily injection level and injection allocation, and the formation pressure continues to decrease, making it difficult to control. Although the surface pump increases the injection volume, efforts toward acidification have been made; the number of under-injection wells is increasing year by year.

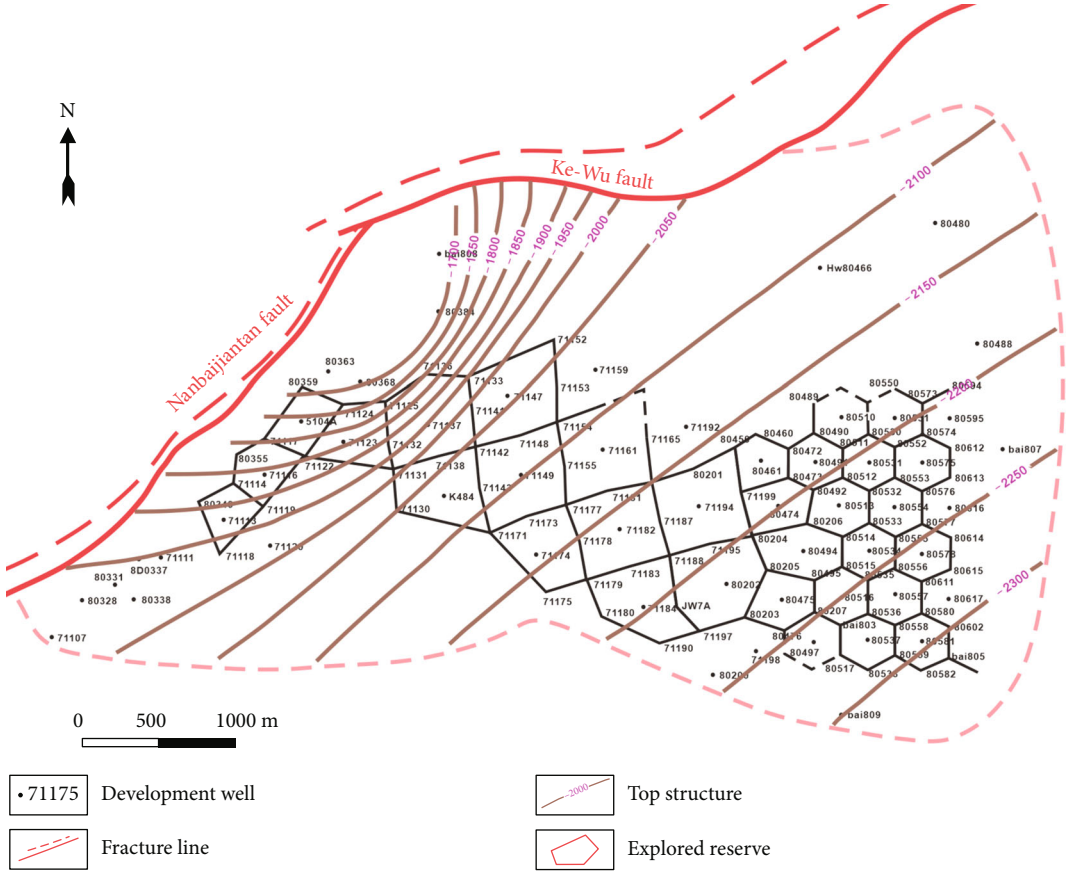

Figure 1: Structural location map of the top surface of the study area.

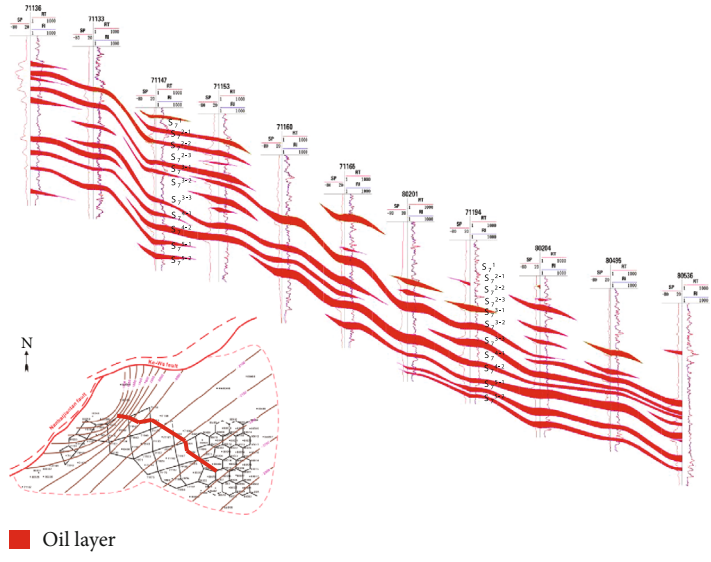

Figure 2: Cross-sectional view of the oil layer of the reservoir.

Furthermore, water sensitivity research has been performed at only a few of cored wells in the study area. Currently, the water sensitivity data are insufficient to determine the water sensitivity in the area. Moreover, cumulative water injection of 21 wells in the study area revealed that injection amounts greatly varied among individual wells. Thus, the reservoir has high heterogeneity, and the differences in water sensitivity are not clearly understood.

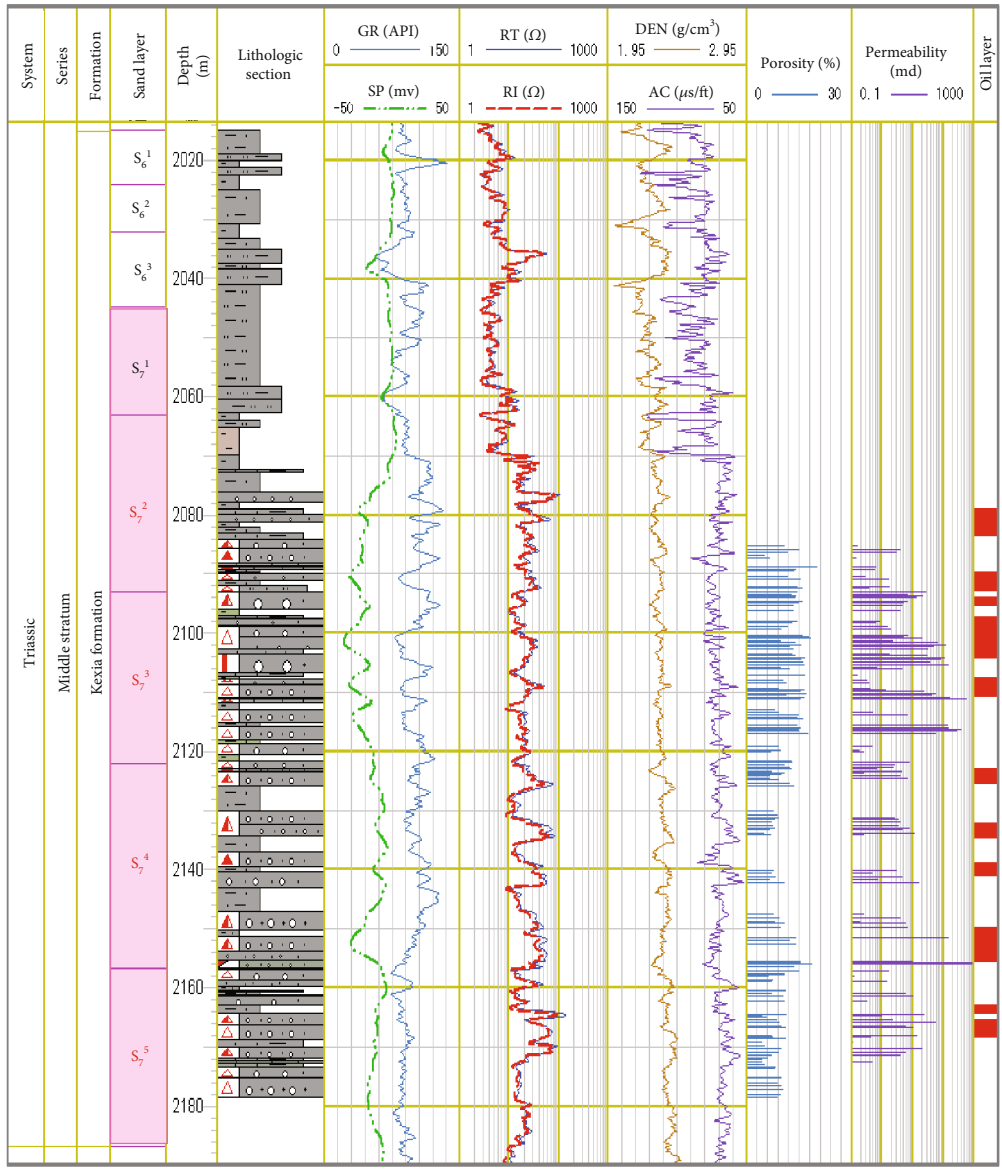

Figure 3: Comprehensive histogram of Well K484.

Table 1: Physical and chemical properties of clay minerals.

Characteristic	Cation exchange capacity (mg/100 g)	Expansibility	Specific surface area (m^2/cm^3)	Relative solubility	
				HCl	HF
Kaolinite	3–15	Nothing	8.8	Slight	Slight
Illite	10–40	Quite weak	39.6	Slight	Slight to moderate
Smectite	76–150	Strong	34.9	Slight	Moderate
Chlorite	0–40	Weak	14	High	High
Illite/smectite	—	Relatively strong	34.9 ~ 39.6	Mutative	Mutative

Therefore, it is necessary to perform an evaluation, interpretation, and distribution study of the water sensitivity of individual wells in the low-permeability conglomerate reservoir in this area.

3. Data Preparation

The physical and chemical properties of clay minerals were summarized according to the book *Clay Mineral and Clay*

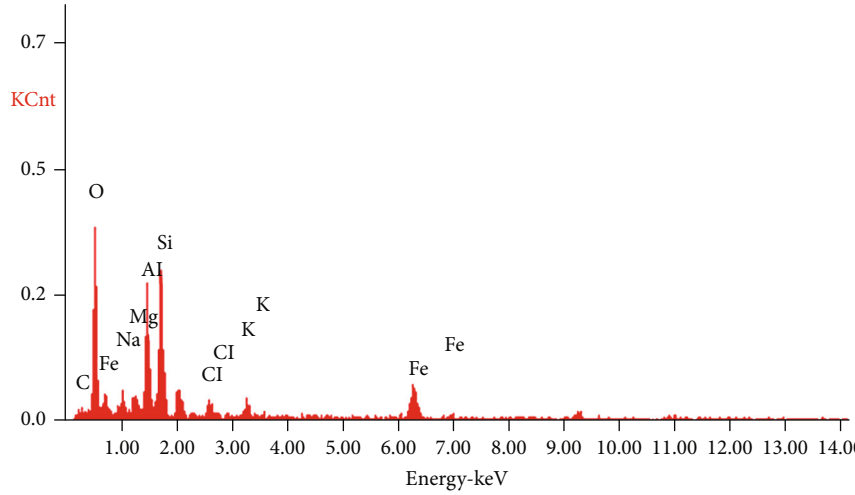

Figure 4: Analysis of clay mineral composition.

Table 2: Statistics on average clay content in each layer.

Stratum	Sample number	I/S mixed layer		Illite		Kaolinite		Chlorite	
		Interval	Mean	Interval	Mean	Interval	Mean	Interval	Mean
S_7^3	63	6–88	36.4	3–43	17.13	6–66	31.77	3–52	16.31
S_7^4	23	1–60	32.04	4–48	23.08	7–52	28.48	7–66	21.15
S_7^5	18	13–73	44.33	3–28	15	5–54	26.21	5–35	16.84

Table 3: Water sensitivity test data of three cores of Well Bai 806.

Well	The sample depth (m)	Sequence number	Salinity of injected water (mg/L)	Pore volume injected (%)	Sample permeability (formation) (mD)	Sample permeability (ionic) (mD)
Bai 806		1	32661.02	10.1	0.0672	0.05853
Bai 806	2592.61	2	16330.51	20.1	0.0457	0.0398
Bai 806		3	0	30.2	0.0274	0.02386
Bai 806		1	32661.02	10.1	0.0787	0.0657
Bai 806	2593.79	2	16330.51	20.1	0.0523	0.04364
Bai 806		3	0	30.2	0.0291	0.02428
Bai 806		1	32661.02	10.1	0.101	0.0648
Bai 806	2595.39	2	16330.51	20.1	0.0584	0.0375
Bai 806		3	0	30.2	0.0334	0.0214

Mineral Analysis (Table 1). By comparing the properties of clay minerals, smectite undergoes the most intense swelling because of water absorption. Therefore, we can infer that water sensitivity-related damage is primarily caused by smectite. Accordingly, illite and chlorite have a small influence, and kaolinite should have almost no water sensitivity. As per XRD experiments, this area contains illite/smectite mixed-layer rather than only smectite. Therefore, in this area, the water sensitivity damage is primarily caused by the water absorption and expansion of the illite/smectite mixed-layer, while illite affects the water sensitivity to some extent.

Table 4: Evaluation table for water sensitivity index.

Water sensitivity index I_w (%)	Intensity of water sensitivity
$I_W \leq 5$	None
$5 < I_W \leq 30$	Weak
$30 < I_W \leq 50$	Medium weak
$50 < I_W \leq 70$	Medium strong
$70 < I_W \leq 90$	Strong
$90 < I_W$	Extremely strong

Table 5: Water sensitivity test data.

Well name	The sample depth (m)	The sample permeability in the formation water condition (mD)	The sample permeability in the ionic water condition (mD)	I_w	Intensity of water sensitivity
T8084	2218.82	5.62	4.93	0.123665	Weak
	2224.87	2.52	2.24	0.110317	Weak
	2227.02	51.2	50.78	0.008262	None
	2229.52	13.2	12.79	0.031667	None
71146	2182.78	1.49	0.97	0.352349	Medium weak
	2258.5	1.44	1.18	0.18125	Weak
	2260.65	5.62	5.37	0.045018	None
	2359.13	1.57	0.74	0.529299	Medium strong
Jian590	2026.36	0.344	0.157	0.543605	Medium strong
	2099.11	0.257	0.1838	0.284825	Weak
Bai 806	2592.61	0.0672	0.05853	0.129018	Weak
	2593.79	0.0787	0.0657	0.165184	Weak
	2595.39	0.101	0.0648	0.358416	Medium weak
T82012	2209.1	0.188	0.07	0.62766	Medium strong
	2213.67	1.55	1.389	0.103871	Weak
	2244.55	12.6	12.314	0.022698	None

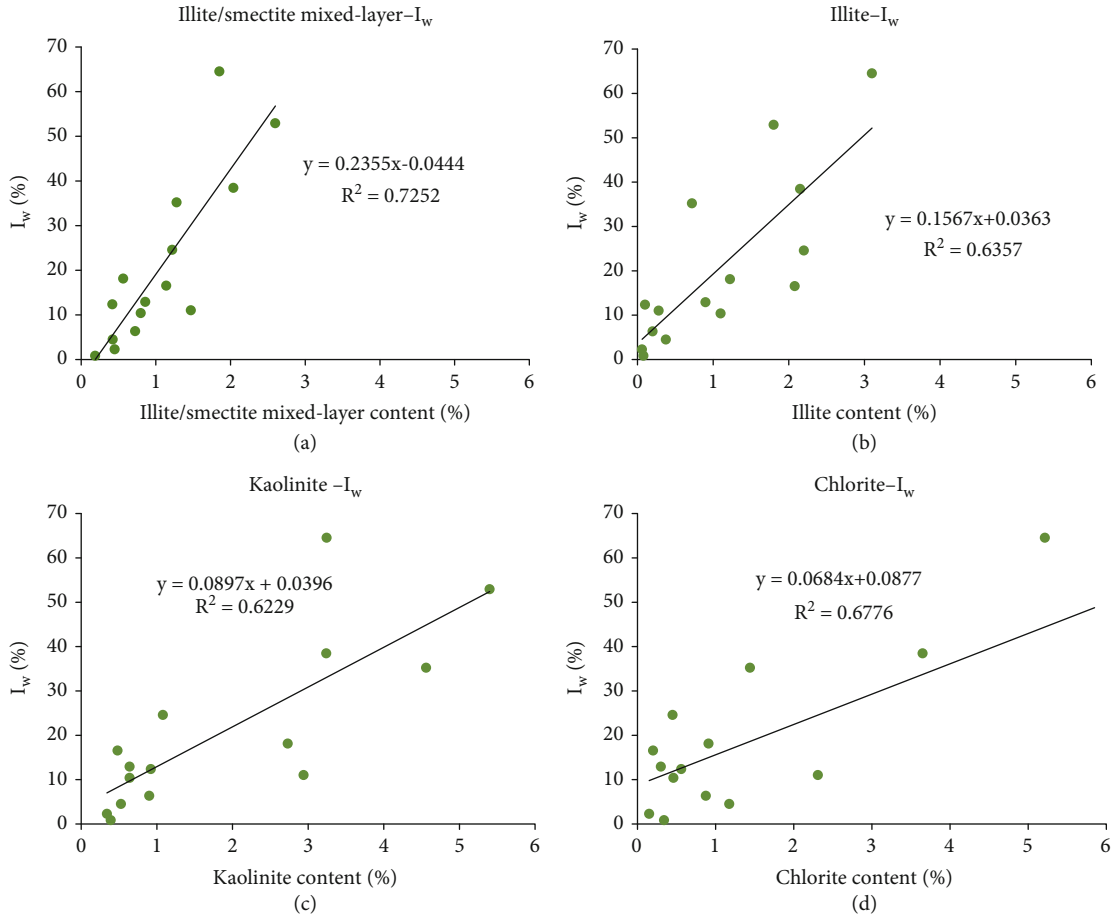

Figure 5: Graphs of relations between various clay minerals and water sensitivity index: (a) illite/smectite mixed-layer–I_w; (b) illite–I_w; (c) kaolinite–I_w; chlorite–I_w.

Table 6: Basic characteristics of conventional clay minerals.

Clay mineral	GR (API)	U (ppm)	Th (ppm)	K (%)	DEN (g/cm^3)	AC (μs/ft)	HI
Smectite	150–200	4.3–7.7	0.8–2.0	0.0–1.5	2.0–2.5	364.96	12
Illite	250–300	8.7–12.4	10–25	3.51–8.3	2.7–2.9	172.41	12
Kaolinite	90–130	4.4–7.0	6–19	0.0–0.5	2.4–2.7	217.39	36
Chlorite	180–250	17.4–36	0–8	0.0–0.3	2.76	179.86	36

Table 7: Statistical correlations between clay minerals and logging parameters.

R^2	φ_N	φ_D	φ_S	Vsh	φ_N/φ_D	φ_S/φ_D	φ_S/φ_N
Illite/smectite	0.3600	0.2611	0.0424	0.1429	0.0059	0.1340	0.2237
Illite	0.4147	0.3069	0.0449	0.1444	0.0262	0.1521	0.2480
Kaolinite	0.2916	0.1417	0.0773	0.1884	0.0123	0.1918	0.1866
Chlorite	0.4083	0.2098	0.0686	0.1815	0.0388	0.1452	0.2873

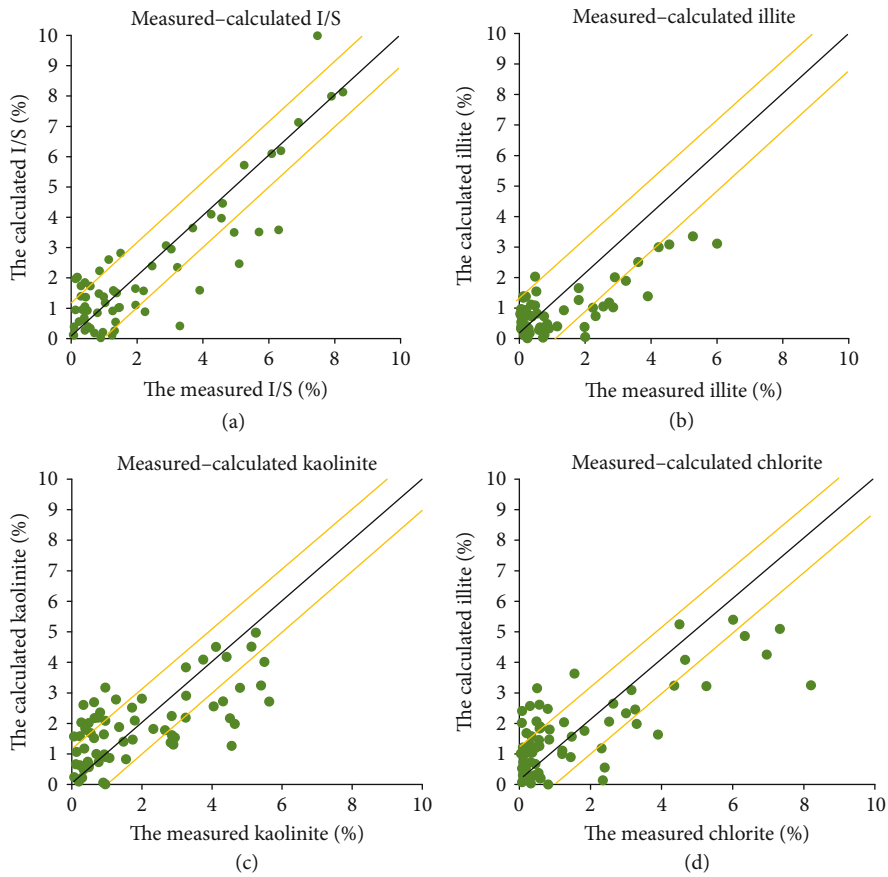

Figure 6: Comparison of measured and calculated clay mineral content predicted by multiple linear regression: (a) measured–calculated I/S; (b) measured–calculated illite; (c) measured–calculated kaolinite; (d) measured–calculated chlorite.

3.1. XRD Diffraction Analysis. For better scientific understanding of the strata in the study area, rock samples were collected and classified in the drilling site; furthermore, representative rock samples were selected for the XRD analysis of mineral composition, and a large amount of information reflecting the characteristics of clay minerals can be provided.

Quantitative XRD analysis of clay minerals can be used to determine the relative content of each mineral in a

mixture. The higher the content of a mineral in a mixed sample, the stronger the intensity of its diffraction peak will be. The diffraction intensity of the mineral is directly proportional to its content in the mixed sample (Figure 4) [11].

Through XRD data analysis, a large number of clay minerals have developed in the reservoir in the study area (Table 2), and the cementation between particles was loose, resulting in particle migration and plugging [10]. With increase in depth, the content of illite/smectite mixed-layer increases, and the content of kaolinite decreases, resulting in a strong reservoir water sensitivity.

3.2. Water Sensitivity Test and Water Sensitivity Index. The water sensitivity index is a quantitative index for evaluating the water sensitivity of reservoirs. As per this index, a larger value indicates a higher water sensitivity. To understand the water sensitivity of the reservoir, a water sensitivity experiment was performed on the core. The specific methods used are as follows. First, 16 core specimens were labeled and oil-washed, and their length, diameter, porosity, and permeability were measured. Then, ionic water samples at 32,661.02, 16,330.51, and 0 mg/L with different salinity flowed through the core; furthermore, the corresponding permeability values were measured, considering the following three samples as examples (Table 3; [25]). Finally, the water sensitivity indices of different rock samples were calculated, and the water sensitivity of rock samples was classified as per the established criteria (Table 4):

The calculation formula for water sensitivity index is listed below:

$$I_W = \frac{K_f - K_i}{K_f} \times 100\%, \quad (1)$$

where I_w is the water sensitivity index, K_f is the permeability of the rock sample under the condition of formation water, and K_i is the permeability of the rock sample under the condition of ionic water [25].

The water sensitivity test results from 16 cores from five wells in the study area are presented in Table 5. Overall, the water sensitivity index ranged from 0.83% to 62.7% and had an average value of 21.7%. The water sensitivity intensity was classified from "none" to "medium strong," while no strong water sensitivity was observed.

3.3. Clay Mineral Content. Using the core XRD analysis data, the rock characteristics were analyzed, thus providing a foundation for the accurate calculation of the contents of different types of clay minerals. To summarize, the relative contents of various clay minerals were obtained from XRD data of 16 cores from five wells. We considered argillaceous content to be the clay mineral content. Therefore, the absolute clay mineral content could be obtained as per the clay content in the core intercalation. The absolute clay mineral contents are the product of argillaceous content and relative contents of clay minerals.

The correlations between the water sensitivity index and each clay mineral were fitted (Figure 5). The illite/smectite mixed-layer had good correlation with the water sensitivity index. Moreover, the illite content had a positive correlation with water sensitivity index; however, the correlations between kaolinite and chlorite and water sensitivity index were poor.

Table 8: Multiple linear regression prediction effect.

	Illite/smectite	Illite	Kaolinite	Chlorite
R	0.712	0.752	0.675	0.736
R^2	0.5078	0.5655	0.4556	0.5417
Error range	±1.2%	±1.2%	±1.2%	±1.2%
Accuracy rate	60.60%	77.27%	62.12%	68.18%

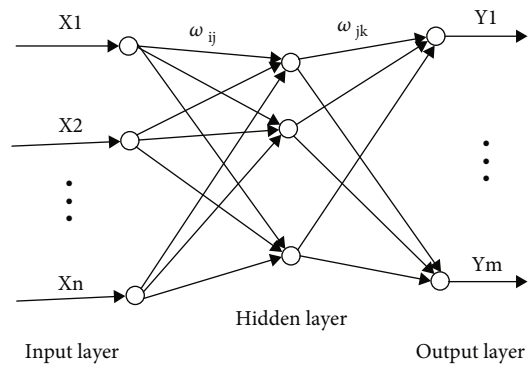

Figure 7: Neural network principles.

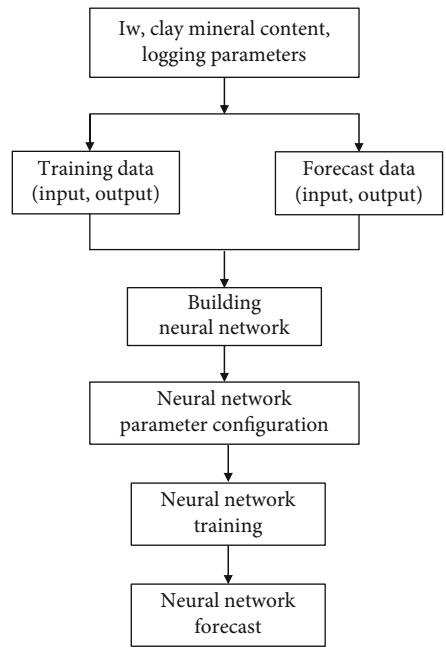

Figure 8: Neural network flow chart.

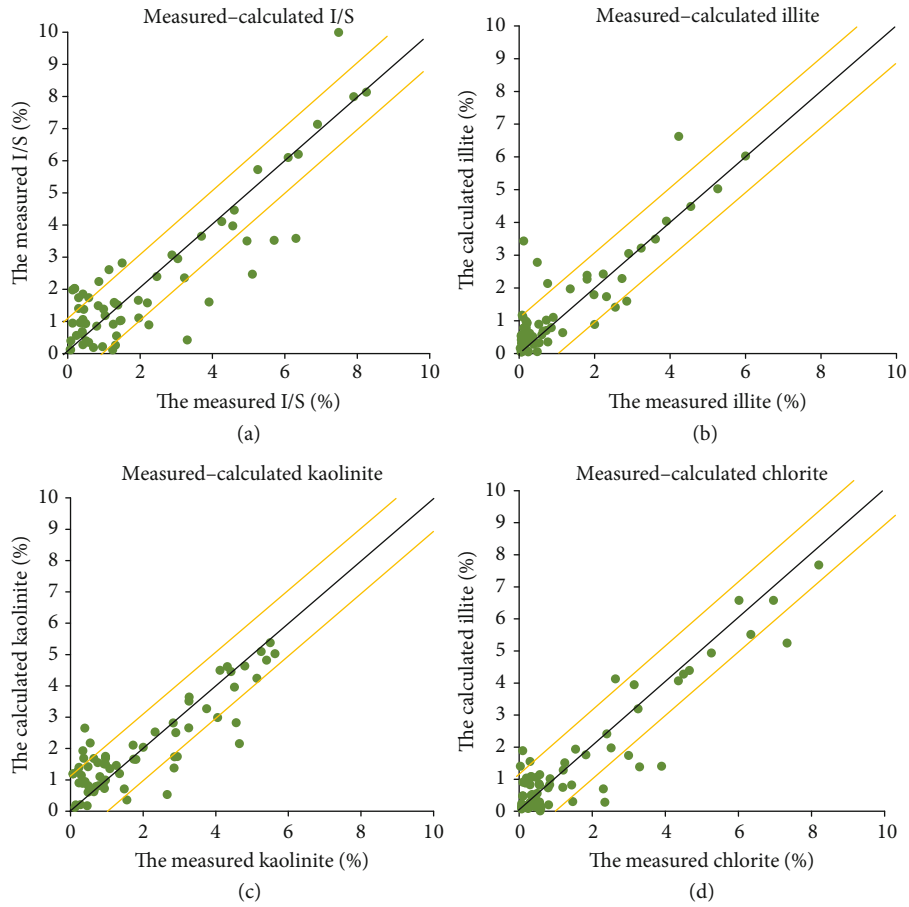

Figure 9: Comparison of measured and calculated clay mineral content predicted by the neural network: (a) measured–calculated I/S; (b) measured–calculated illite; (c) measured–calculated kaolinite; (d) measured–calculated chlorite.

3.4. Logging Parameter Selection. Using an in-depth study of the basic characteristics of conventional clay minerals (Table 6), the four types of clay mineral had considerable differences in terms of neutrons, density, sonic transit time, natural gamma ray spectra, cation exchange capacity, and other characteristics [17].

In multiple oil fields, it is extremely difficult to calculate the content of clay minerals because most wells do not provide natural gamma ray spectral data. Therefore, to build the calculation model, only natural gamma ray (GR) data, neutrons (CNL), density (DEN), and sonic transit time (AC) could be used. To mitigate differences caused by different data attributes in the analysis, the abovementioned data were quantified without rigidity. Note that neutron, density, and sonic transit time log values were converted to neutron porosity (φ_N), density porosity (φ_D), and sonic porosity (φ_S), respectively; furthermore, the natural gamma ray log values were converted to argillaceous content (Vsh). Moreover, the variables φ_N/φ_D, φ_S/φ_D, and φ_S/φ_N were introduced [17].

The neutron, density, and sonic transit time log values were converted into the corresponding porosities using the following formulas:

Table 9: Neural network prediction effect.

	Illite/smectite	Illite	Kaolinite	Chlorite
R	0.8780	0.8768	0.8669	0.9170
R^2	0.7710	0.7687	0.7516	0.8408
Error range	±1.2%	±1.2%	±1.2%	±1.2%
Accuracy rate	75.76%	93.94%	87.88%	87.88%

$$\varphi_N = \frac{\varphi_N - \varphi_{Nma}}{\varphi_{Nf} - \varphi_{Nma}}, \tag{2}$$

$$\varphi_D = \frac{\rho_{Nma} - \rho_b}{\rho_{Nma} - \rho_f}, \tag{3}$$

$$\varphi_S = \frac{\triangle t - \triangle t_{Nma}}{\triangle t_{Nf} - \triangle t_{Nma}}. \tag{4}$$

φ_{Nf} is the hydrogen index of the fluid, φ_{Nma} is the skeleton hydrogen index, ρ_f is the fluid density (g/cm^3), ρ_{Nma} is the skeleton density (g/cm^3), $\triangle t_{Nf}$ is the fluid sonic transit

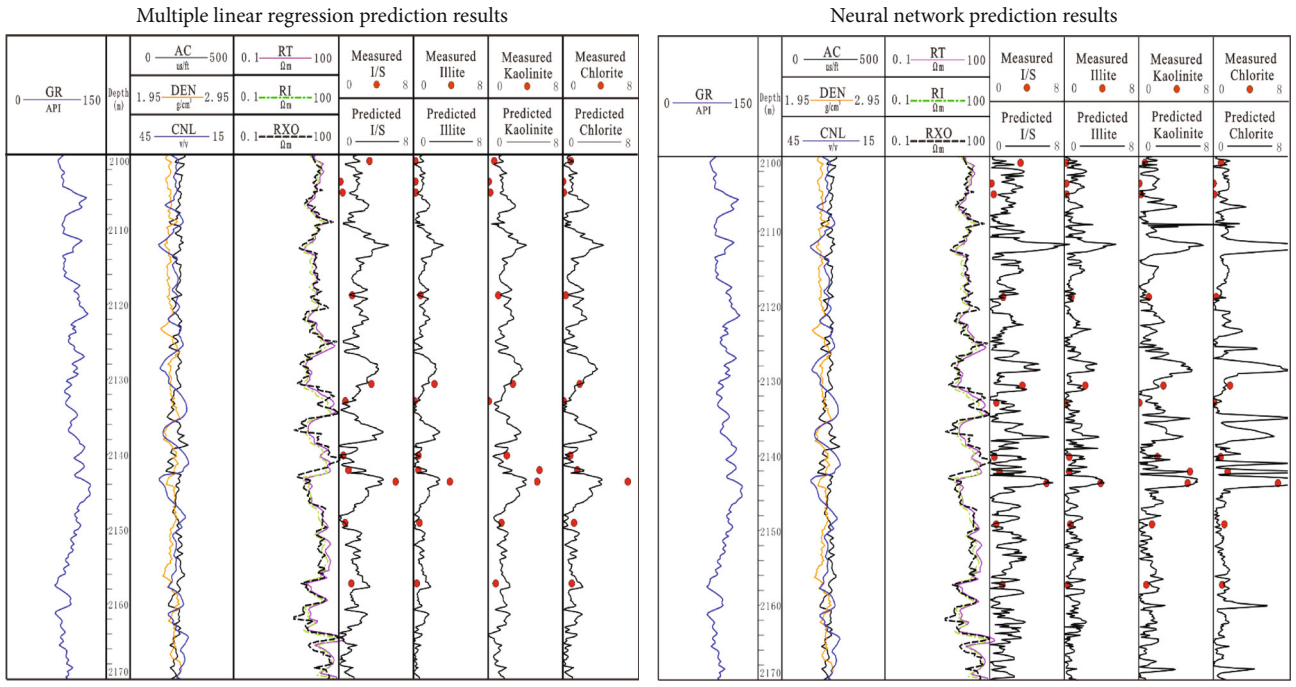

Figure 10: Method comparison: (a) multiple linear regression prediction results; (b) neural network prediction results.

Table 10: Comparison of clay mineral content prediction accuracy.

Accuracy rate	Illite/smectite	Illite	Kaolinite	Chlorite
Multiple linear regression	60.60%	77.27%	62.12%	68.18%
Neural network	75.76%	93.94%	87.88%	87.88%

time (μs/m), and $\triangle t_{Nma}$ is the skeleton sonic transit time (μs/m).

The core and clay mineral content data of 66 sample points in five wells were differentiated and collected for the following analysis.

4. Methods

4.1. Method for Quantitative Interpretation of Mineral Content. The core analysis data of 66 sample points from five wells on the seven logging parameters were analyzed using a single correlation analysis to form the correlation coefficient matrix (Table 7). The overall correlation was reported to be poor using certain data that exhibited good correlation. An improved correlation can be considered to correspond to sensitive clay mineral logging parameters.

4.1.1. Multiple Linear Regression Analysis. Regression analysis measures general relationships between dependent variables and independent variables correlated as per a correlation analysis [26]. For practical geological problems, many independent variables often work together to influence dependent variables. Furthermore, multiple linear regression uses the best-fitting straight line (regression line) to establish a relationship between dependent variable (Y) and multiple independent variables ($X1$, $X2$, and $X3$). We used herein multiple linear regression to establish a model of the relationship between clay minerals and their corresponding sensitive logging parameters to quantitatively explain the clay mineral content.

Using data analysis, the quantitative prediction model of each clay mineral was gradually regressed as follows:

$$V_{I/S} = 19.565 \times \varphi_N + 19.699 \times \varphi_D - 2.999 \times \frac{\varphi_S}{\varphi_N} - 3.543, \quad (5)$$

$$V_I = 13.559 \times \varphi_N + 13.548 \times \varphi_D - 1.852 \times \frac{\varphi_S}{\varphi_N} - 3.027, \quad (6)$$

$$V_K = 20.697 \times \varphi_N - 2.033 \times \frac{\varphi_S}{\varphi_D} + 1.245 \times \mathrm{Vsh} - 1.301, \quad (7)$$

$$V_C = 20.805 \times \varphi_N + 10.548 \times \varphi_D - 2.623 \times \frac{\varphi_S}{\varphi_N} + 1.415 \times \mathrm{Vsh} - 3.523. \quad (8)$$

The clay mineral content can be predicted using the abovementioned formulae. The predicted clay mineral content was compared with the measured clay mineral content;

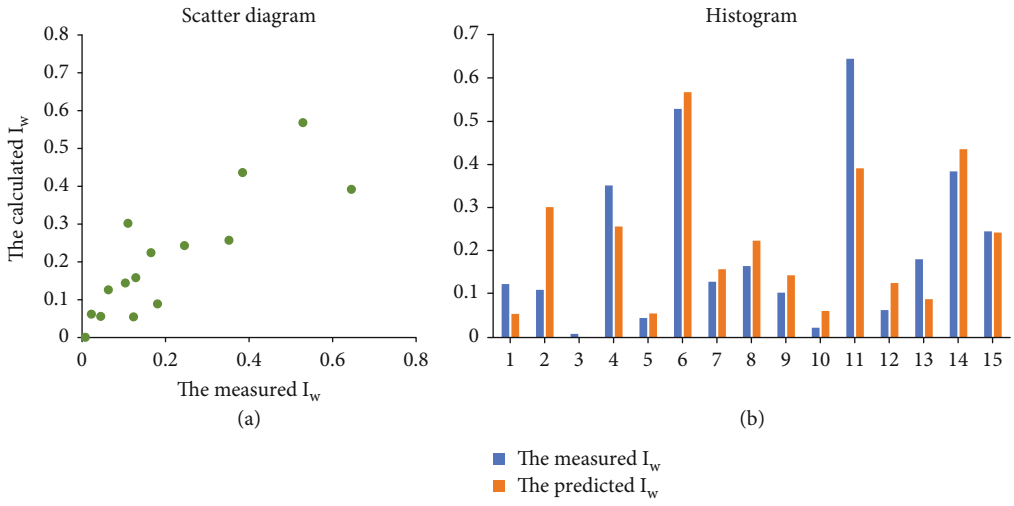

Figure 11: Comparison of measured I_w and predicted I_w: (a) scatter diagram; (b) histogram.

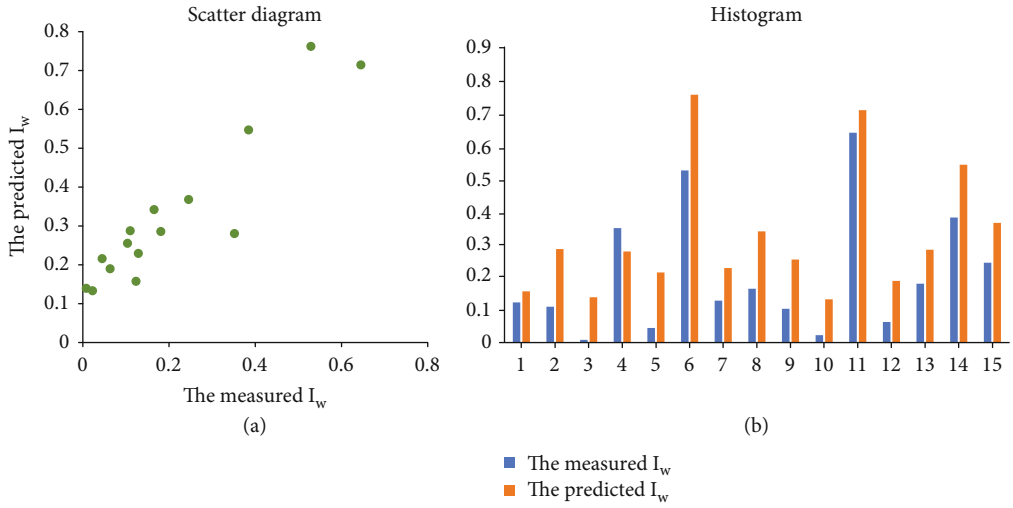

Figure 12: Comparison diagram of measured I_w and predicted I_w: (a) scatter diagram; (b) histogram.

moreover, a scatter plot was drawn. Considering the straight line $y = x$ as a standard, the accuracy was determined to be in the range of a 1.2% fluctuation (Figure 6, Table 8).

4.1.2. Neural Network Analysis. The accuracy of the multiple linear regression method is not extremely high. Thus, a method for establishing the relationship between logging parameters and clay minerals is proposed based on the use of a neural network (NN).

An NN is an "operation model" [27] that does not require a mathematical equation stating a mapping relationship between the input and output to be determined in advance. It instead learns rules or relations through its own training process to obtain a result closest to the expected output value when the input value is provided, converting N input vectors to M component output vectors. The primary characteristic of NNs is that, during transmission, the input signal is processed layer by layer. Accordingly, the input layer passes via the hidden to output layers, and each layer of neurons only affects the state of the next layer of neurons. If the output layer does not obtain the expected output, the network weight along with various other parameter configurations will be adjusted to achieve a predicted output close to the expected output value [28, 29].

Generally, an NN is a nonlinear and adaptive information processing system composed of a large number of processing units. Similar to an intelligent information processing system, the core of an artificial neural network is an algorithm. The basic principle is given below (Figure 7, [18, 27]).

$X_1, X_2, \cdots, X_n$ is the input value of the neural network, $Y_1, Y_2, \cdots, Y_m$ is the predicted value of the network, both ω_{ij} and ω_{jk} are the weight of the network.

Here, the NN input value was set based on the sensitive logging parameters of 66 core samples from five standard wells (T8084, T82012, Bai 806, 71146, and 71116; Table 7),

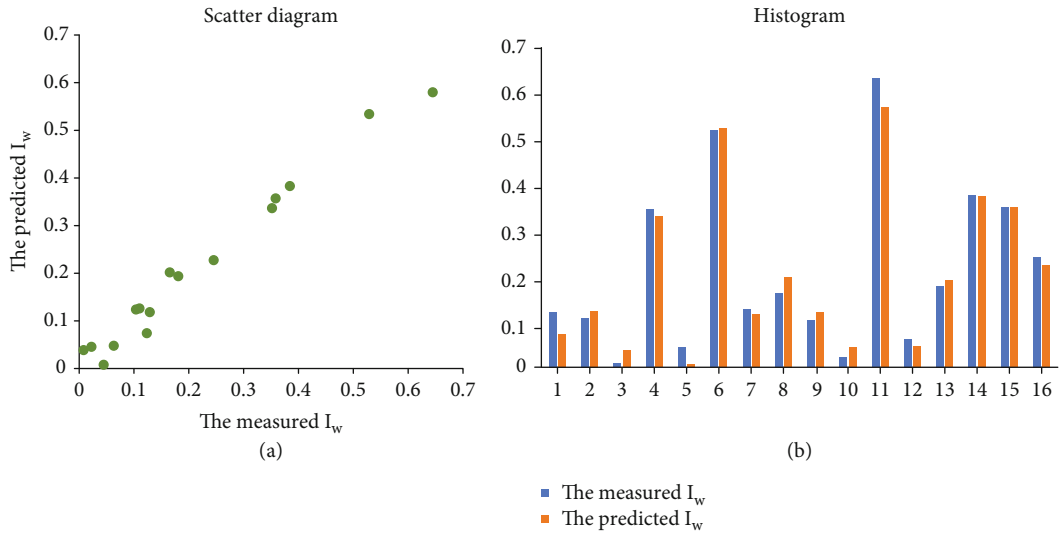

Figure 13: Comparison diagram of measured I_w and predicted I_w: (a) scatter diagram; (b) histogram.

and the output value was the clay mineral content of the corresponding depths. The logging parameters of 78 wells in the study area were used to train the NN, and the quantitative relationship between the input and output was obtained. This was then used to predict the content of various clay minerals in other wells.

The basic process of the NN method is listed below (Figure 8).

On the basis of depth correction, training and prediction data are first read. Then, the following processes are employed:

(1) *Network Parameter Configuration*. The network parameters are set as per the actual situation of the study area, e.g., the samples were randomly divided as follows: 70% of samples were selected as test data, 15% of samples were selected as validation data, and 15% of samples were selected as testing data. The number of hidden neurons was 10

(2) *NN Training*. The input value of the sample is fit to the output value

(3) *NN Prediction*. The logging parameter part of the sample to be predicted is entered to predict the clay mineral content [27]

Logging curves with good correlation with each mineral were selected to fit the clay mineral content in turn. The fitting relation obtained by NN during training is used to predict clay mineral content. Then, the predicted clay mineral content is compared with the measured content, and a scatter chart is drawn. Considering the straight line $y = x$ as a standard, the accuracy was determined to be within a range of a 1.2% fluctuation (Figure 9 and Table 9).

4.1.3. Method Comparison. By comparing the accuracy of these two methods, multiple linear regression calculation of clay mineral content was affected by multiple variables, and its accuracy was low (Figure 10 and Table 10). Furthermore, the NN machine learning method exhibited a strong correlation and high accuracy between the clay mineral prediction and measured clay minerals. Thus, in the study area, the NN method can be considered as the preferred method for clay mineral log interpretation.

Table 11: Comparison table of water sensitivity index prediction accuracy.

Methods	Accuracy rate
Single factor linear regression	43.75%
Multiple linear regression	12.50%
Neural network	93.75%

4.2. Water Sensitivity Index Interpretation Method. As per the absolute content of clay minerals in the 16 cores from the five wells, the relationship between the water sensitivity index and absolute clay mineral content was analyzed along with the water sensitivity test data. Graphs demonstrating the contents of four types of clay minerals in relation to water sensitivity index were then established. By comparing the relationship between the four clay minerals and water sensitivity index, a larger coefficient leads to a greater contribution to water sensitivity. However, a smaller one leads to a lower contribution. The linear regression equations of these four types of clay minerals and the water sensitivity index were obtained as follows:

$$I_w = 0.2355 \times V_{I/S} - 0.0444, \quad (9)$$

$$I_w = 0.1567 \times V_I + 0.0363, \quad (10)$$

$$I_w = 0.0897 \times V_K + 0.0396, \quad (11)$$

$$I_w = 0.0684 \times V_C + 0.0877, \quad (12)$$

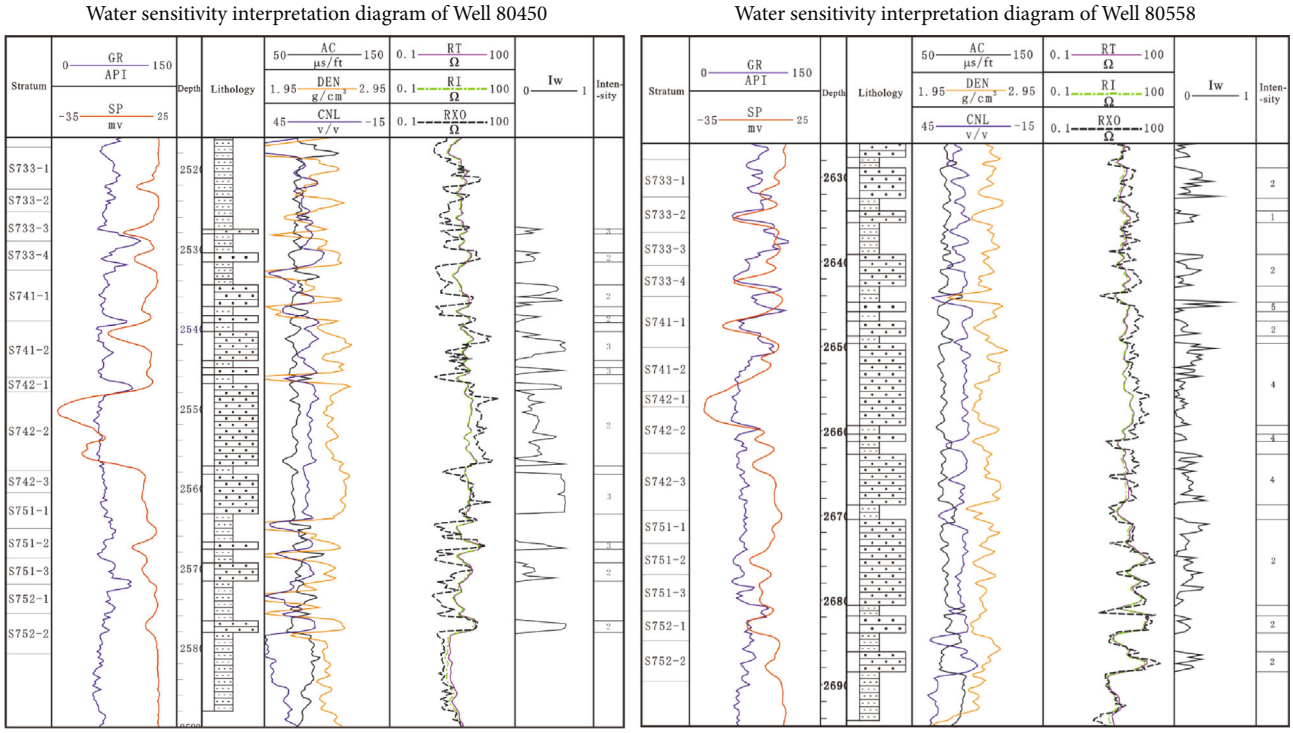

Figure 14: Individual well water sensitivity interpretation diagram: (a) water sensitivity interpretation diagram of Well 80450; (b) water sensitivity interpretation diagram of Well 80558.

where I_w is the water sensitivity index, $V_{I/S}$ is the illite/-smectite mixed-layer content, V_I is the illite content, V_K is the kaolinite content, and V_C is the chlorite content.

4.2.1. Single-Factor Linear Regression Method. Single-factor linear regression uses the best-fit straight line (known as the regression line) to establish a relationship between the dependent variable (Y) and an independent variable (X). The illite/smectite mixed-layer is the main mineral affecting water sensitivity. The single-factor linear regression method was used to establish the relationship between the water sensitivity index I_w and the illite/smectite mixed-layer to calculate the water sensitivity index I_w. The fitting formula used was $I_w = 0.2355 \times V_{I/S} - 0.0444$. Using this formula to predict the water sensitivity index and comparing the predicted water sensitivity index with the measured one, the errors of the seven points were within ±0.05 in the 15 samples, and the accuracy rate was 43.75% (Figure 11).

4.2.2. Multiple Linear Regression. Generally, multiple linear regression is more effective and useful than single-factor linear regression for prediction or estimation. Because kaolinite has almost no water sensitivity, the relational model between water sensitivity index I_w and the other three clay minerals was established using multiple linear regression to calculate the water sensitivity index I_w. The fitting formula used to predict the water sensitivity index was $I_w = 0.021 \times V_{I/S} + 0.095 \times V_I + 0.042 \times V_C + 0.11$. By comparing the predicted water sensitivity index with the measured water sensitivity index, in 15 samples, only two points had an error within ±0.05; however, their accuracy was 12.50% (Figure 12).

4.2.3. Neural Network Analysis. In terms of the clay mineral interpretation, only input and output data used were the water sensitivity index and clay mineral content, respectively. Furthermore, we used MATLAB for the NN operations. The water sensitivity index and water sensitivity mineral data of 16 sample points in five wells were input as two variables into MATLAB. The NN then used these for training to obtain a better correlation for the system with the aim of predicting the water sensitivity index. Comparing the predicted water sensitivity index with the measured water sensitivity index, out of the 16 samples, 15 points had an error within ±0.05, and the accuracy rate was 93.75% (Figure 13).

4.2.4. Method Comparison. Based on a comparative analysis of the accuracy of the abovementioned methods (Table 11), the NN machine learning method yielded a stronger correlation between the predicted and the measured water sensitivity index while the accuracy was high. Therefore, the NN machine learning method can be considered the preferred method for predicting the water sensitivity index in the research area.

4.3. Predicting Outcomes. Based on the above prediction method, clay mineral content was used as the medium to interpret the water sensitivity intensity, and 1,223 reservoir intervals from 78 wells in the study area were interpreted.

Two particular wells are obtained as examples (Figure 14). In this figure, 1 represents no water sensitivity, 2 represents weak sensitivity, 3 represents medium-to-weak sensitivity, 4 represents medium-to-strong sensitivity, 5 represents strong sensitivity, and 6 represents extremely strong sensitivity.

5. Conclusion

This study introduces the use of an NN in the interpretation of water sensitivity logs. A linear regression and an NN were used to calculate the clay minerals and water sensitivity index of glutenite in the Lower Karamay Formation in the 530-well area of District 8 in the Karamay oil field. The following conclusions were drawn:

(1) In the absence of natural gamma ray spectral data, gamma, neutron, density, and sonic log data can be used to establish a clay mineral content model

(2) The NN model was able to retain details on clay mineral changes when calculating clay mineral content in this area as well as calculate the water sensitivity index values. This makes it possible to more accurately represent the changes in the water sensitivity of the formation. Compared with multiple linear regression, the NN method has a number of obvious advantages. The prediction results agree with the water sensitivity test results; furthermore, the accuracy rate was high, indicating this method can provide a more realistic basis for future exploration and development

Data Availability

The data that support the findings of this study are available on request from the corresponding author.

Conflicts of Interest

The authors declare that they have no conflicts of interest.

Acknowledgments

This work was financially supported by the Science Foundation of China University of Petroleum, Beijing (grant number 2462020YXZZ022).

References

[1] R.-F. Krueger, *An overview of formation damage and well productivity in oilfield operations*, Society of Petroleum Engineers, 1988.

[2] L. Song, R. Zhu, D. Zhu, S. Sui, and C. Zhou, "Influences of clay minerals on physical properties sandstones of Xujiahe formation in Guang'an area," *Journal of Southwest Petroleum University (Science & Technology Edition)*, vol. 33, pp. 73–78 +11-12, 2011.

[3] X. Zheng, *Study on log evaluation of clay mineral and water sensitivity for shale gas reservoir*, China University of Petroleum, Beijing, 2018.

[4] Z. Chen, S. Zhang, and M. Shen, *Potential damages of clay minerals in oil-field protection*, Journal of the Chengdu Institute of Technology, 1996.

[5] C.-H. Hewitt, *Analytical techniques for recognizing water-sensitive reservoir rocks: reservoir rock analyses*, Reservoir Rock Analyses, 1963.

[6] C. S. Land, "Effect of hydration of montmorillonite on the permeability - to gas of water-sensitive reservoir rocks," *Journal of Petroleum Technology*, vol. 17, no. 10, pp. 1213–1218, 1965.

[7] J. Liu, Y. Kang, R. Chen, D. Liu, J. Yang, and J. He, "Present research situation and developing trend of formation damage mechanism and protection technology for carbonate rocks," *Petroleum Geology and Recovery Efficiency*, vol. 13, pp. 99–101, 2006.

[8] R.-N. Valdya and H. S. Fogler, "Fines migration and formation damage: influence of pH and ion exchange," *Society of Petroleum Engineers SPE Production Engineering*, vol. 7, no. 4, pp. 325–330, 1992.

[9] S.-R. Bishop, *The Experimental Investigation of Formation Damage Due to the Induced Flocculation of Clays within a Sandstone Pore Structure by a High Salinity Brine*, Society of Petroleum Engineers, 1997.

[10] Y. Kang and P. Luo, *Influence of clay minerals on formation damage in sandstone reservoir – a review and prospect*, Drilling Fluid and Completion Fluid, 2000.

[11] F. Sun, W. Sun, Z. Hou, and L. Wang, *X-Ray Analysis Method for Measurement of Clay Minerals Content*, Conservation and Utilization of Mineral Resources, 2013.

[12] Y. Wang, "The method of application of gamma-ray spectral logging data for determining clay mineral content," *Journal of Oil and Gas Technology*, vol. 35, pp. 100–104+2, 2013.

[13] Q. Shi, *Preliminary investigation on quantitative analysis of the composition of clay minerals using NGS log*, Well Logging Technology, 1998.

[14] S. Yong and C. Zhang, *Logging data processing and comprehensive interpretation*, China University of Petroleum Press, Dongying, 1996.

[15] K. Blnnyan and Q. P. Passey, "Clay estimation from Gr and neutron -density porosity logs," *Society of petrophysicists and well-log analysts*, vol. 10, pp. 43–50, 1994.

[16] Q. Huang, J. Liu, and Z. Wang, *The application of natural gamma-ray logging data in determining the content of clay minerals*, Journal of Jilin University, 2007.

[17] P. Xing, J. Sun, K. Wang, Z. Li, and J. Wu, "Comparison of determination methods for clay minerals using log data," *Journal of China University of Petroleum*, vol. 32, pp. 53–57, 2007.

[18] X. Ma and J. Li, "Predicting clay composition in shale by neural network modeling," *Drilling Fluid and Completion Fluid*, vol. 10, pp. 20–46, 1993.

[19] C. Peng and J. Yan, "Applications of artificial neural network in predicting formation sensitivity: petroleum drilling," *Techniques*, vol. 25, pp. 16–20, 1997.

[20] Z. Zhang, K. Han, D. Yu, and Z. Zhang, "Using support vector machine to forecast reservoir sensitivity," *Well Logging Technology*, vol. 29, pp. 308–310, 2005.

[21] X. Zhao and Y. Zhang, *Analysis of Clay Minerals and Clay Minerals*, Ocean Press, Beijing, 1990.

[22] Z. Liu, G. Liu, C. Zhou, L. Song, C. Li, and H. Zhang, *A Method for Determining the Triporosity Logging Parameters of Dry*

Clay and a Method for Manufacturing the Device: CN104632202B, Beijing sanyou intellectual property agency co. LTD, 2014.

[23] H. Xu, *Study on Conglomerate Reservoir Characteristics and Adjustment Countermeasures of Well Block 530 in Block 8 of Karamay Oilfield*, Southwest Petroleum University, 2013.

[24] J. Han, B. Li, S. Guo, T. Wang, and Y. Zhu, "Research on the integration of progressive exploration and development of conglomerate reservoir," *Inner Mongolia Petrochemical Industry*, vol. 41, pp. 129–132, 2015.

[25] J. Liao, H. Tang, X. Zhu, M. Ren, Z. Sun, and D. Lin, "Water sensitivity experiment and damage mechanism of sandstone reservoirs with ultra-low permeability: a case study of the eighth oil layer in the Yanchang Formation of Xifeng oilfield, Ordos Basin," *Oil & Gas Geology*, vol. 33, pp. 321–328, 2012.

[26] B. Zhu, "Developing support software for rapidly predicating the formation-sensitivity with analytic method of single correlation and multiple regression," *Science Technology and Engineering*, vol. 12, pp. 8617–8621, 2012.

[27] H. Lu, Q. Li, D. Yue et al., "Study on optimal selection of porosity logging interpretation methods for Chang 7_3 segment of the Yanchang Formation in the southwestern Ordos Basin, China," *Journal of Petroleum Science and Engineering*, vol. 198, p. 108153, 2021.

[28] J. Lin, H. Li, N. Liu, J. Gao, and Z. Li, "Automatic lithology identification by applying LSTM to logging data: a case study inX tight rock reservoirs," *IEEE Geoscience and Remote Sensing Letters*, vol. 18, pp. 1361–1365, 2020.

[29] N. Liu, T. He, Y. Tian, B. Wu, J. Gao, and Z. Xu, "Common-azimuth seismic data fault analysis using residual UNet," *Interpretation*, vol. 8, no. 3, pp. SM25–SM37, 2020.